September 1999 • NREL/SR-520-26566

Subcontractor Report

Atmospheric Pressure Chemical Vapor Deposition of CdTe for High Efficiency Thin Film PV Devices

Annual Report
26 January 1998—25 January 1999

P.V. Meyers
ITN Energy Systems — Wheat Ridge, Colorado

R. Kee, C. Wolden, L. Raja, V. Kaydanov, T. Ohno, R. Collins, M. Aire, and J. Kestner
Colorado School of Mines — Golden, Colorado

A. Fahrenbruch
ALF, Inc. — Stanford, California

National Renewable Energy Laboratory

1617 Cole Boulevard
Golden, Colorado 80401-3393

NREL is a U.S. Department of Energy Laboratory
Operated by Midwest Research Institute • Battelle • Bechtel

Contract No. DE-AC36-98-GO10337

September 1999 • NREL/SR-520-26566

Atmospheric Pressure Chemical Vapor Deposition of CdTe for High Efficiency Thin Film PV Devices

Annual Report
26 January 1998—25 January 1999

P.V. Meyers
ITN Energy Systems — Wheat Ridge, Colorado

R. Kee, C. Wolden, L. Raja, V. Kaydanov, T. Ohno, R. Collins, M. Aire, and J. Kestner
Colorado School of Mines — Golden, Colorado

A. Fahrenbruch
ALF, Inc. — Stanford, California

NREL Technical Monitor: H.S. Ullal

Prepared under Subcontract No. ZAK-8-17619-03

National Renewable Energy Laboratory

1617 Cole Boulevard
Golden, Colorado 80401-3393

NREL is a U.S. Department of Energy Laboratory
Operated by Midwest Research Institute • Battelle • Bechtel

Contract No. DE-AC36-98-GO10337

NOTICE

Available to DOE and DOE contractors from:
Office of Scientific and Technical Information (OSTI)
P.O. Box 62
Oak Ridge, TN 37831
Prices available by calling 423-576-8401

Available to the public from:
National Technical Information Service (NTIS)
U.S. Department of Commerce
5285 Port Royal Road
Springfield, VA 22161
703-605-6000 or 800-553-6847
or
DOE Information Bridge
http://www.doe.gov/bridge/home.html

 Printed on paper containing at least 50% wastepaper, including 20% postconsumer waste

Table of Contents

1 Project objective

ITN's three year project Atmospheric Pressure Chemical Vapor Deposition (APCVD) of CdTe for High Efficiency Thin Film PV Devices has the overall objectives of improving thin film CdTe photovoltaic (PV) manufacturing technology and increasing CdTe PV device power conversion efficiency. Tasks required to accomplish the overall goals are grouped into 1) development of APCVD apparatus and procedures which enable controlled deposition of device-quality film over large area and 2) development of advanced measurement and analytical procedures which provide useful and effective device characterization.

1.1 Approach

CdTe deposition by APCVD employs the same reaction chemistry as has been used to deposit 16% efficient CdTe PV films, i.e., close spaced sublimation, but employs forced convection rather than diffusion as a mechanism of mass transport. Tasks of the APCVD program center on demonstration of APCVD of CdTe films, discovery of fundamental mass transport parameters, application of established engineering principles to the deposition of CdTe films and, verification of the reactor design principles which could be used to design high throughput, high yield manufacturing equipment. Additional tasks relate to improved device measurement and characterization procedures which can lead to a more fundamental understanding of CdTe PV device operation. Specifically, under the APCVD program, device analysis goes beyond conventional one-dimensional device characterization and analysis toward two dimension measurements and modeling.

1.1.1 Deposition technology

Although there are many demonstrated methods for producing high-efficiency CdTe solar cells, large-scale commercial production of thin-film CdTe PV modules has not yet been realized.[1] An important contributor to the commercial production of thin-film CdTe will be development of advanced deposition reactors. APCVD represents a generation beyond close spaced sublimation (CSS) – the technology which has produced the highest efficiency CdTe PV cells to date.[2,3] APCVD combines proven CSS reaction chemistry with state-of-the-art engineering principles to enable design of thin film deposition reactors for the manufacturing environment. APCVD's anticipated advantages include:

- Low equipment cost compared to vacuum processing because equipment will need neither the structural strength nor the pumping systems of a vacuum chamber.
- Large area uniformity is achieved through control of temperature and gas flow - both of which are subject to rigorous engineering design.
- Simplified process control and source replenishment because the source gas generation is physically separated from the deposition chamber.
- CdTe PV device fabrication process compatibility in that APCVD is presently used commercially to deposit transparent conducting oxide (TCO) films commonly used in CdTe solar cells. In fact, the processing sequence: deposit TCO, deposit CdS, deposit CdTe, dry $CdCl_2$ heat treatment and metalorganic CVD of electrodes could be performed in a single continuous process.
- Low raw material costs as CdTe is used in its least expensive form - chunks.
- Simplified continuous processing because gas curtains replace load locks.

1.1.2 Device analysis

Operation of thin film PV devices is normally analyzed in one dimension – distance perpendicular to the device surface. One dimensional (1D) modeling is justified in that thin film PV devices are basically comprised of a stack of thin films of various compositions and properties and through which light and electricity flow in a direction essentially perpendicular to the plane of the films. There is no question that 1D modeling successfully describes the fundamentals of thin film PV device operation. Nonetheless, quantitative analysis of PV device operation, its dependence on device fabrication procedures, and factors affecting stability in the field have not been achieved. Furthermore, we know that individual films are not homogeneous, but rather are comprised of grains. Each grain is surrounded by grain boundaries that are oriented in all directions and which have different physical, electrical and optical properties than does the interior of the grain. Thus tasks of this program are directed toward techniques for quantifying the properties of grain boundaries and for quantifying effects grain boundaries may have on thin film PV device operation.

An important distinction between the commonly used one dimensional (1D) models and a two dimensional (2D) model is that the 2D model allows for electric fields and carrier transport both parallel and perpendicular to the direction from which light is incident. These perpendicular components are brought about by differences in carrier type, carrier concentration, and carrier lifetime associated with grain boundaries. In this project efforts are being directed toward the experimental characterization of grain boundaries and the investigation of the effects of these characteristics on working devices. An important aspect of this approach is maintenance of a close connection between measurement, modeling and analysis.

2 APCVD

2.1 Background

2.1.1 Reaction chemistry

CdTe film deposition by CSS or APCVD is a three-step process that involves (i) generation of elemental vapors, (ii) vapor transport, and (iii) condensation and reaction to form CdTe. Congruent sublimation of CdTe occurs through the reaction

$$CdTe + heat \leftrightarrow Cd(g) + \frac{1}{2} Te_2(g) . \qquad (1)$$

Vapor pressure over solid CdTe in a chemically inert environment depends only on temperature and is described by the Antoine equation

$$log\,[P_{sat}] = 6.823 - 10{,}000/T \quad . \qquad (2)$$

where T is temperature Kelvin and saturation pressure, P_{sat}, is expressed in atmospheres. In both APCVD and CSS, Cd and Te_2 vapors are transported to a substrate that is maintained at a somewhat lower temperature than the source. At the substrate temperature, the source gas is supersaturated causing Cd and Te_2 vapors to react and form CdTe. The degree of supersaturation and the rate of material delivery to the surface determine deposition rate. Cd and Te_2 can also condense to form their elemental condensed phases, but at all temperatures the elemental vapor pressures of Cd and Te_2 over their respective condensed phases is much higher than either gas over CdTe. Figure 1 displays possible reaction mechanisms which may occur on the growing CdTe film surface. In practice, for substrates held above ~500°C and deposition rates ~ 5 μm/min the deposited films are single phase CdTe.

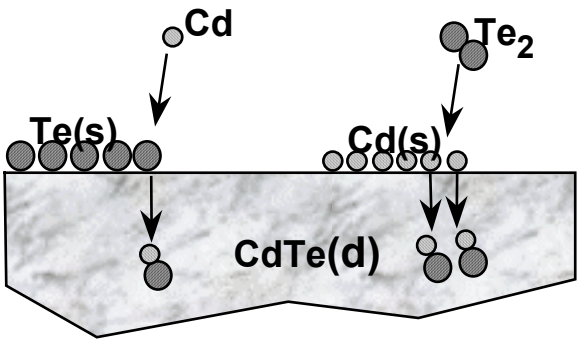

Figure 1 Possible CdTe deposition mechanism - Eley-Rideal mechanism. On the left side Cd(g) atoms react with condensed Te to form CdTe before the Te can re-evaporate. The analogous process – with Te_2(g) reacting with momentarily condensed Cd, is displayed on the right side.

It is emphasized that these reactions depend only on temperature and on the concentrations of the source gases immediately above the superstrate. In particular, the reactions do not depend upon the pressure of inert gases such as N_2, Ar or He. Thus the heterogeneous reaction chemistry, i.e., the set of reactions that take place on the substrate, is the same for CSS, elemental vapor deposition, or APCVD. The primary difference between CSS and APCVD is the mechanism of mass transport.

2.1.2 Mass transport

2.1.2.1 Diffusion

Mass transport of the gas source species occurs through a combination of diffusion and convection. Most previous work, including CSS and elemental vapor deposition, has been performed in closed systems where diffusion is the lone transport mechanism. Mass flux due to diffusion is proportional to the product of concentration gradient and diffusion coefficient. In CSS, the concentration gradient is determined by the difference between the equilibrium partial pressures at the source and superstrate and by the physical separation between them.[4] For typical CSS conditions (P = 10-50 torr, source-superstrate spacing of 3-10 mm, and temperature differences of 10-80°C) deposition rates are on the order of 4 μm/min. Use of CSS at atmospheric pressure has been demonstrated, but deposition rates were in the 0.2 μm/min range.[5]

2.1.2.2 Forced convection

Mass transport rate can be increased and control improved over that achieved by diffusion alone by using forced convection. Convection processes are critical in APCVD for both generating elemental vapors and for transporting material to the substrate. Vaporization of source material occurs in a packed bed containing CdTe chunks as illustrated in Figure 2. Mass transport from a packed bed is an efficient and well-characterized method of producing source material-laden gases.[6] Flow in packed beds is turbulent, creating high mass transport coefficients. Partial pressure of CdTe vapors, P_{CdTe}, coming out of the source gas generator is given by

$$P_{CdTe}/P_{sat} = (1-\exp\{- h_m * A_{p,t} * \varepsilon /[v_o * A_{c,b}]\})$$

where P_{sat} is the equilibrium partial pressure at the bed temperature (Eq. 2), $A_{p,t}$ is the total surface area of the particles in the packed bed, $A_{c,b}$ is the cross sectional area of the bed, h_m is the mass transfer coefficient, v_o is the "open velocity" of the gas (i.e., the velocity the gas would have if there were no particles in the bed), and ε is the void fraction of the bed. Calculations for the case of a 10 cm diameter bed packed with ~4 kg of 1 cm diameter particles, maintained at 1000 K (727 °C), and a gas flow rate of 7.6 l/s indicate that the outlet gas will be >99% saturated and the pressure drop will be ~4.5 psi. Source

gas of this throughput and saturation level is sufficient to coat a 100 cm^2 superstrate with 10 µm of CdTe in one minute

Source gas is convected to the deposition chamber via transport piping. Deposition onto piping walls is retarded by heating them to temperatures above the packed bed temperature.

2.2 First year (1998) reactor fabrication progress

During Phase I an APCVD reactor was designed, all components were constructed and assembly was nearly completed. In order to verify reactor performance a "dry run" (operation of reactor without CdTe) was performed. Although the reactor performance was close to that predicted, some deficiencies were discovered. Modifications to the original design are expected to be minor and the APCVD reactor program is expected to be back on schedule in the second year of the program.

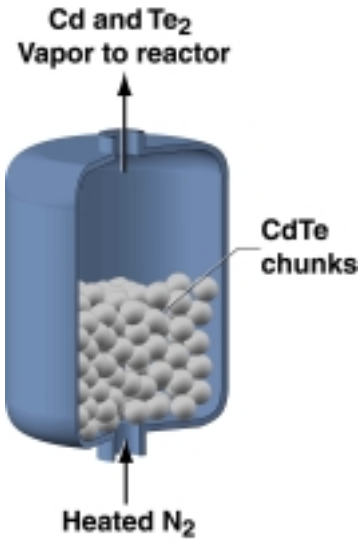

Figure 2 Schematic of the "packed bed" source gas generator

2.2.1 Adopted stagnant flow APCVD reactor concept

A design team consisting of engineers and scientists from ITN and CSM considered various design options for the APCVD reactor. Although all design options involved atmospheric pressure reactors and mass transport by forced convection, the design team considered many possible configurations. Fundamental design issues to be resolved included issues such as: whether source gas flow should be top-down or bottom-up, whether source gas flow would be generally parallel or perpendicular to the substrate surface, whether flow should be turbulent or laminar, and whether gas injectors should be large or small or round or square. After consideration of these various issues, the design team selected the Stagnant Flow Reactor (SFR) design concept, an example of which is displayed in Figure 3.

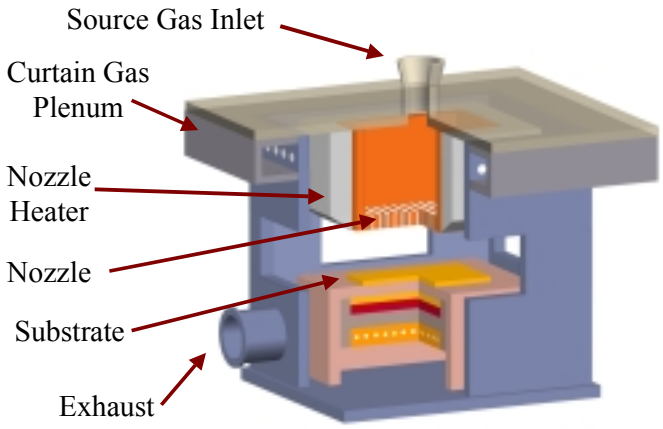

Figure 3 Conceptual stagnation flow reactor which displays the essential features of the APCVD reactor for deposition of thin film CdTe.

SFR design features include a nozzle with an area greater than the substrate out of which the source gas flows uniformly over the nozzle area ($cm^3/s*cm^2$). The nozzle face is parallel to the substrate surface and gas flow from the nozzle is laminar (non-turbulent). Source gas flow is perpendicular to the plane of the surface creating a layer of essentially stagnant gas above the substrate. Considerations which led the design team to adopt the SFR concept at this stage of the project included:

- SFR design enables uniform deposition rate over the substrate surface
- Stagnant Flow Reactors are used commercially in many CVD processes
- Planar geometry allows 1-D simulation of reactor performance
- SFR design enables determination of engineering parameters required for next-generation commercial scale APCVD reactor design

2.2.2 Developed APCVD "stagnant flow" reactor design

Having adopted the SFR design concept, the design team proceeded to design a reactor suitable for APCVD of CdTe. Components of the APCVD reactor are shown schematically in Figure 4. Deposition takes place in a cold wall reactor with a design specification for the source gas of 800ºC. Hot source gas flows laminarly downward and impinges perpendicularly onto the heated substrate at a nominal speed of 50 cm/s. Eddy currents are eliminated and reactor walls are kept cool by a curtain gas which flows parallel to the source gas but outside of and on all four sides of the nozzle. The curtain gas also serves to prevent deposition onto reactor walls.

Substrate temperature control is achieved through a specially designed substrate support which includes both a 500 W heater and water cooling. Inclusion of both heating and cooling capabilities enables active temperature control of the substrate within the temperature range expected during deposition. Specifically, heat can be supplied in order to keep the substrate at the desired temperature - expected to be in the range of 550ºC to 625ºC - but heat from the source gas can be removed under conditions when the source gas transfers excess heat to the substrate.

Compressed nitrogen is used both as the carrier gas for the Cd and Te_2 vapors and as the curtain gas. Before entering the CdTe bubbler (i.e., the packed bed containing chunks of CdTe), carrier gas is preheated to approximately the temperature of the CdTe chunks. Carrier gas passes upward through the CdTe chunks in the packed bed structure (see Figure 2) where Cd and Te_2 gasses are picked up by the carrier gas - creating the source gas for CdTe deposition.

Partial pressures of Cd and Te_2 gasses leaving the bubbler are expected to be close to the equilibrium partial pressure at the bubbler temperature. Source gas can be characterized by its "saturation temperature", T_s, which is determined by solving equation (2) for temperature given the actual Cd and Te_2 gas partial pressures. Thus $T_s \leq T_{bubbler}$. After passing through the packed bed the source gas is transported to the reactor through hot piping. Transport tubing walls are kept at a temperature greater than T_s in order to prevent deposition onto tubing walls.

As a safety precaution the APCVD system is designed to operate slightly below room pressure by a few inches of water (pressure). Thus, after passing through the reactor, exhaust gas is drawn out the deposition zone by a blower (pump) with sufficient capacity to maintain negative partial pressure everywhere in the APCVD system from the exit of the bubbler to the exhaust blower. Before reaching the blower, however, gas exiting the reactor chamber first passes through a heat exchanger and a high efficiency particle accumulator (HEPA) filter which serve to cool and clean the exhaust gas, respectively. Note that any residual Cd and Te_2 gasses remaining in the exhaust gas will deposit onto the cold, i.e., room temperature, walls of the heat exchanger or will be captured as particulates by the HEPA filter. As an additional safety precaution, the entire reactor system will be contained within an enclosed plexiglass

chamber (not shown) which will also be kept at negative pressure with respect to room ambient and will be vented through a second HEPA filter and out of an exhaust duct.

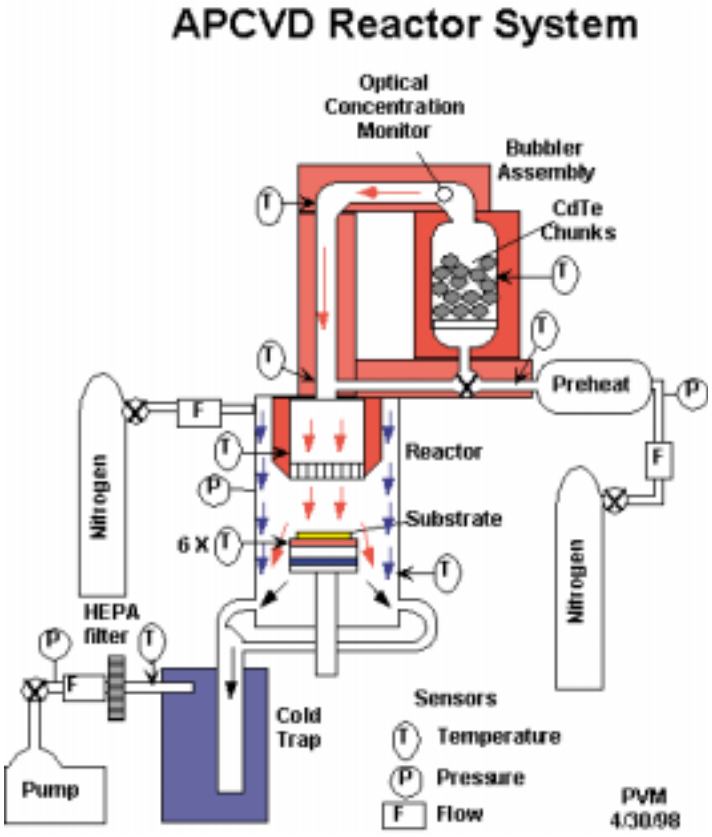

Figure 4 Schematic representation of the APCVD reactor system.

In order to monitor reactor performance, pressure, temperature and flow will be continuously measured at various locations on both the inlet and exhaust sides of the reactor. Temperature, pressure an flow data will be recorded automatically by an HP Data Acquisition Unit and stored on a computer.

2.2.3 Performed numerical simulations of reactor performance

Researchers modeled reactor temperature and flow using computer programs which numerically solved the Navier-Stokes equations using boundary conditions appropriate to the APCVD reactor. An example, shown in Figure 5, shows the temperature distribution and flow streamlines for a specified set of process parameters. Note in particular the uniformity of temperature across the substrate and the absence of eddy currents within the deposition zone.

The hot, flowing, source gas transfers heat, momentum (pressure), and material to the substrate. Each form of transport has its characteristic boundary layer - i.e., thermal, momentum and mass - which are related to one another, but are not identical. For example in the case of film deposition rate, although the majority of mass transport of Cd and Te_2 from the bubbler to the substrate is by forced convection, Cd and Te_2 must make the final 1 - 2 mm of their trip to the substrate by diffusion through the stagnation layer. Figure 6 shows calculated mass fraction and temperature profiles above the substrate for certain assumed process conditions and surface reaction chemistry. Surface reaction chemistry and growth can be characterized by the probability that a gas molecule striking the substrate will react to form

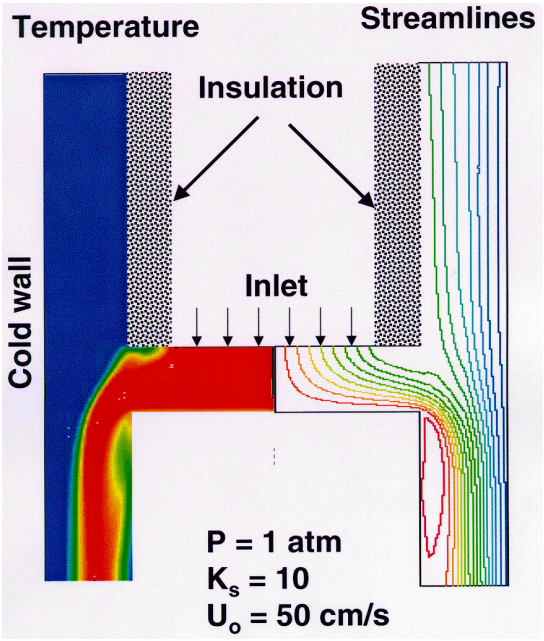

Figure 5 Simulated temperature distribution and gas flow streamlines in the APCVD SFR design. The substrate is directly below the inlet

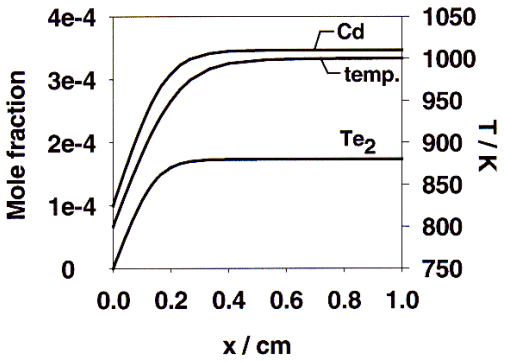

- $T_{bubbler}$ = 1000 K
  U_{inlet} = 100 cm/s; T_{sub} = 800 K
- $Z_{Cd(s)}$ = 0.9995 $Z_{Te(s)}$ ~ 0
  growth rate = 0.34 μm/min
  heat to substrate = 0.524 W/cm^2

Figure 6 Concentration and temperature dependence on distance above substrate for specified assumptions.

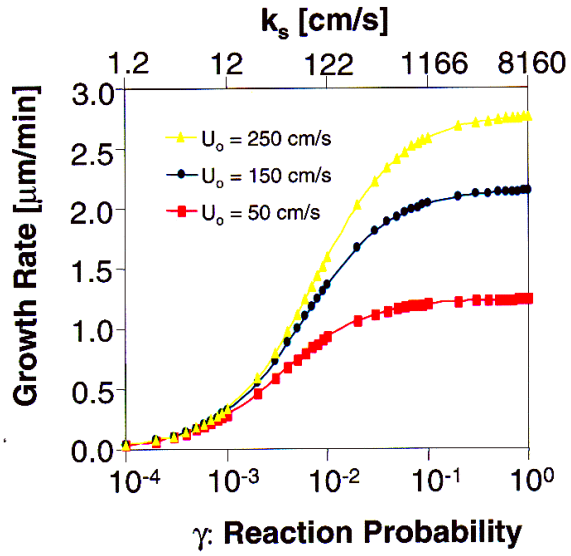

Figure 7 CdTe film growth rate as a function of reaction probability for various nozzle gas velocities.

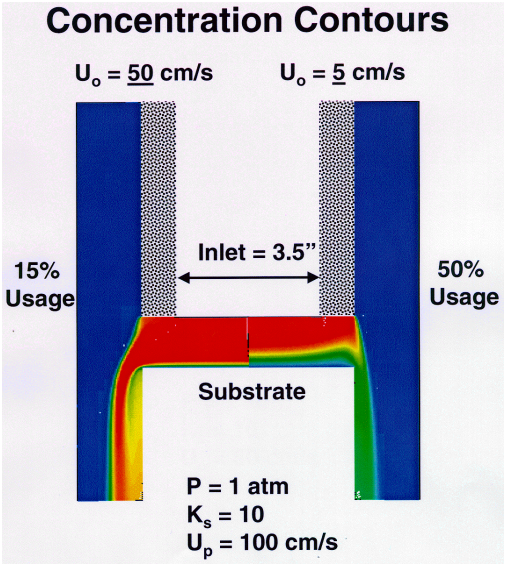

Figure 8 Concentration contours showing carrier gas concentrations and material utilization efficiency for two values of nozzle gas velocity.

CdTe. Figure 7 shows results of a calculation of deposition rate as a function of boundary layer thickness and the rate of chemical reaction at the surface. Modeling has been carried further to simulate growth rate and material utilization efficiency in the present APCVD reactor design. It can be seen in Figure 8 that

the simulated film deposition rate and film uniformity improve with source gas velocity, while material utilization efficiency is higher for lower gas flow. Simulations will be compared with experimental deposition runs in order to better establish mass and thermal transport coefficients and thereby to improve our ability to model reactor performance.

2.2.4 Fabricated APCVD reactor

ITN engineers, with support from the CSM design team, prepared detailed engineering drawings, specified required components, and ordered required parts. CSM and ITN personnel assembled the

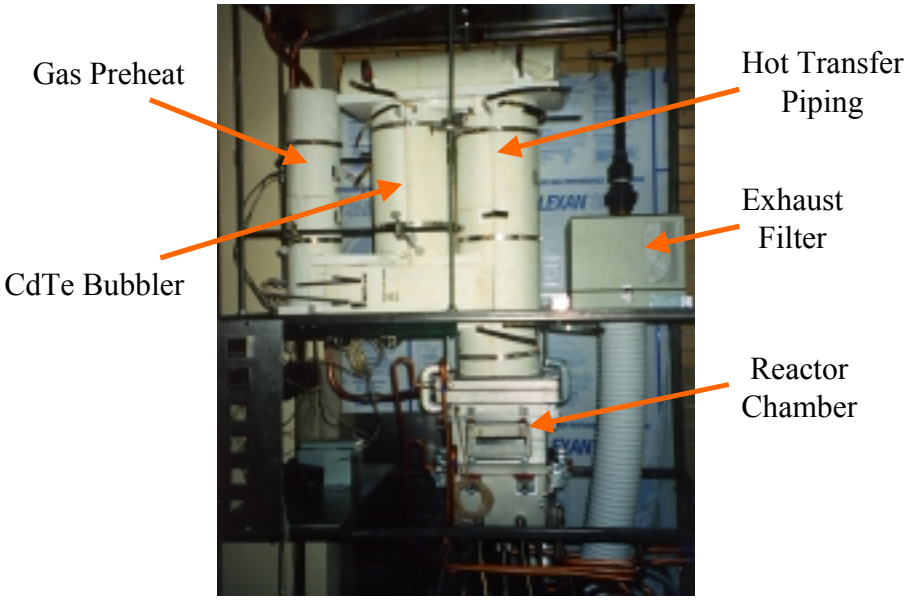

Figure 9 APCVD reactor system as it appeared at the end of the first year of the program.

APVCD components and installed the reactor in the CdTe deposition lab in the Physics Department building at CSM. Figure 9 displays the APCVD reactor as it appeared at the end of 1999.

2.2.5 Performed "dry runs" of reactor to evaluate and document reactor performance

By the end of this first year of the program researchers had begun trials of reactor performance to determine whether design specifications had been achieved. Evaluations runs were performed "dry", i.e., without CdTe in the bubbler, in order to avoid contamination of reactor components in the event that the reactor would require redesign or re-assembly. During the dry runs gas flow and pressure were monitored as well as temperature at all key points. Figure 10 shows representative temperature acquired during a dry run.

Gas supply, water cooling, temperature control, exhaust gas blower, process monitors and data acquisition were all evaluated and found to work generally as expected.

Although the dry run was generally successful in that the required gas flows and temperatures were readily achieved, the dry run also identified certain deficiencies in the reactor design. Specifically, it was discovered that there were certain "cold spots" in the hot piping system and that gas exiting the nozzle was only about 650ºC. In addition, not all sensors performed as required. Although the remedy for these deficiencies is straightforward, researchers decided not to operate the reactor until these deficiencies have been successfully addressed.

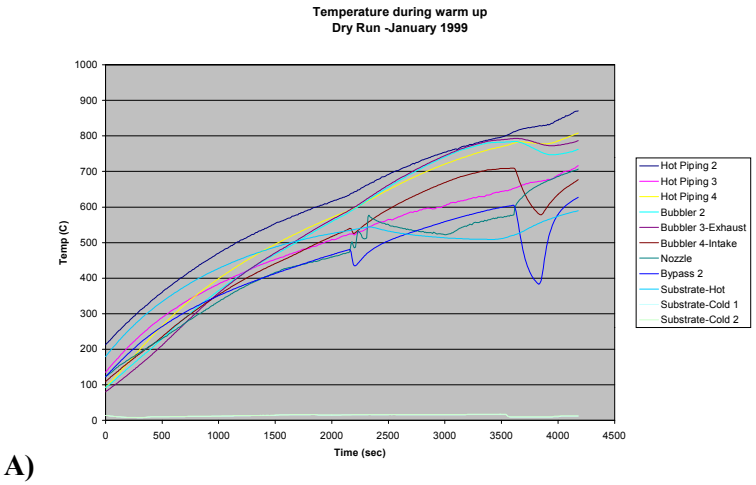

A)

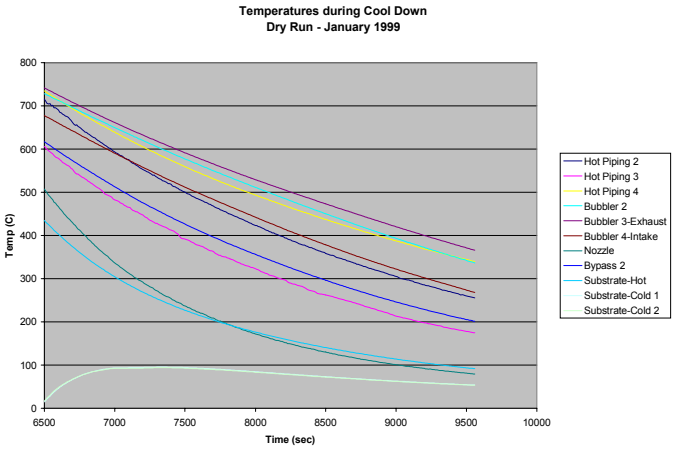

B)

Figure 10 Representative graphs showing temperature data recorded during A) heat-up and B) cool-down portions of the APCVD reactor dry runs.

2.3 APCVD reactor plans

ITN first task of the second year of the APCVD program will be to correct the deficiencies of the existing reactor. Additional heating zones will be installed and all sensors will be made to operate correctly. Results of these modifications will be evaluated during a second set of dry runs.

As soon as reactor performance has been verified, CdTe film depositions and characterization studies will begin. Initial runs will evaluate the reactor performance space through a series of designed experiments which will establish the dependencies of film growth and film parameters on deposition procedure and process parameters. Actual reactor performance will be compared with simulated performance to establish more accurate values for mass and thermal transport parameters. Growth rate, thickness uniformity, and CdTe film structure will be monitored to determine the relationships between process parameters and film characteristics. Additional film characterization will include optical transmission, SEM micrographs, in-plane AC impedance, Seebeck coefficient, and radio frequency photoconductivity measurements as required.

Device fabrication will be central to evaluation of film properties. CSM researchers will use their facilities to produce CdS layers, and back electrodes and to perform other processes required to produce CdTe/CdS PV devices. Light and dark I-V, C-V, QE, and near field scanning optical microscopy

(NSOM) photoconductivity measurements will be utilized, as necessary, to characterize PV devices. Film and device characterization will be performed at ITN, CSM or NREL, as appropriate and available.

Specific milestones for reactor performance during the second year of the program include:

- Demonstration of device quality films
- Demonstration of 12% device conversion efficiency

3 Modeling of CdS/CdTe thin film solar cells

3.1 Modeling approach

Modeling of thin-film CdS/CdTe solar cells using the program AMPS-1D[7] has been done to visualize the relationships between the many variables involved.[8] These 1D simulations are steps toward 2D modeling of the effects of grain boundaries in polycrystalline (PX) cells. Modeling begins with duplication of the experimentally observed cell parameters Voc, Jsc, and ff using a cell structure and materials parameters as close those of champion cells as possible.

Present and future investigations are being focused on several aspects of the solar cell structure:

(a) Front layer - Effects of thickness and properties of CdS and transparent conducting oxide (TCO) layers and of CdS/CdTe interface recombination

(b) Cd and Te interdiffusion - How CdSTe alloys at the CdS/CdTe interface and at the CdTe grain boundaries affect the cell parameters

(c) Depletion layer – How depletion layer width in the CdTe layer affects cell parameters

(d) CdTe layer - Effects of thickness, doping gradients, and minority carrier lifetime in the CdTe, Effects of polycrystallinity and grain boundaries

(e) Back contact - Effects of a potential barrier at the back contact and its relation to stressing the cell

3.2 Purposes of modeling

This section of the report focuses on definition of the problem and on some modeling results on the front layer and the CdTe layer. Modeling results on the back contact are presented elsewhere.[9]

Because of the complexity of simultaneous solution of the transport and continuity equations for electrons and holes for a two terminal device, only the simplest of cases can be done symbolically, i.e., in closed form. For more complex devices, solutions are best obtained using numerical solution techniques. The major value of such models is not in prediction, but as an *experimental tool* for evaluation of measured device performance. Numerical simulations enable the researcher to:

1. visualize fields, potentials, currents, regions of high recombination, and effects of light and dark on carrier transport,
2. identify material properties and device structure parameters that have strong or weak effects on the cell operation,
3. develop ideas that can be tested experimentally,
4. compare effects of process variations on measured device properties with expected effects on device properties predicted by the simulations.

3.3 Modeling resources

Electronic transport modeling programs available commercially and from Universities vary from quite simple 1D programs that run on PCs (with minimal cost) to complicated, expensive 2D and 3D programs that run on minicomputers and work stations. The former programs are considerably more user friendly than the later group. Simulations presented here were done using AMPS-1D.[7]

Our experience with AMPS shows the following :

1. AMPS has an intuitive and straight forward graphical user interface, with an excellent plotting facility.
2. AMPS is reasonably fast (25 min/case at 300 MHz, 64 MB RAM).
3. The AM1.5 spectrum is built in.
4. AMPS will handle devices with many layers.
5. AMPS handles multiple sets of recombination centers with different energies, densities, and lifetimes. It supports either a lifetime approach or specification of energy level, cross sections and densities, so it can handle p/i/n structures where the charge on the recombination centers can have a strong effect.
6. Data sets generated are very comprehensive (conduction band, (CB), valence band, (CV), and electron and hole Fermi levels, (E_{Fn}, E_{Fp}), electric field, recombination, generation, n, p, trapping, J_n, J_p, J_{total}, light, and dark J-V, and more).
7. There is no provision for external series resistance (e.g., grids), tunneling, or internal reflectance (e.g., at the CdS/CdTe interface).

3.4 Definition of the problem

A modeling procedure for CdS/CdTe cells might progress from a simple 1D layered structure with no grain boundaries to a 2D approximation of one cylindrical grain, for which grain boundaries play a role.

The 1D layered structure treated here is shown in Figure 11, with the CdTe subdivided into layers to simulate the grading of acceptor density (and possibly lifetime) thought to be inherent in the polycrystalline cells.

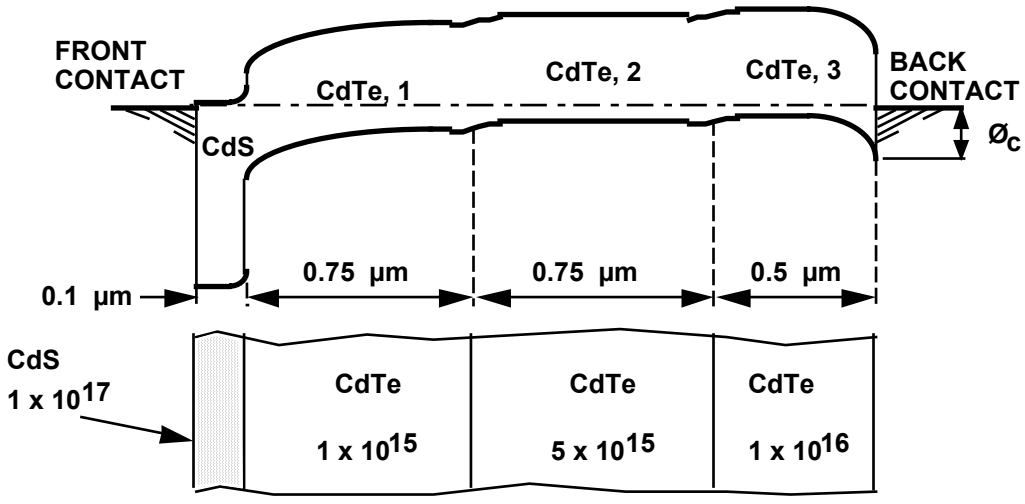

Figure 11 Band diagram and layer structure for "basis" case

To extend the analysis to two dimensions, a cross section of a more realistic polycrystalline device is shown in Figure 12, where interdiffusion of S and Te at the CdS/CdTe interface and grain boundaries, as well as Cu diffusion from the back contact, is included. Since each CdTe grain is roughly cylindrical, the cell can be approximated by a system of idealized grains, one of which shown in Figure 13. One could then proceed to model the 2D grain of Figure 13, using the insight provided by the previous results for 1D to gain insight to the effects of polycrystallinity. To study the cell "system" one would appropriately combine the results for a variety of grain sizes.

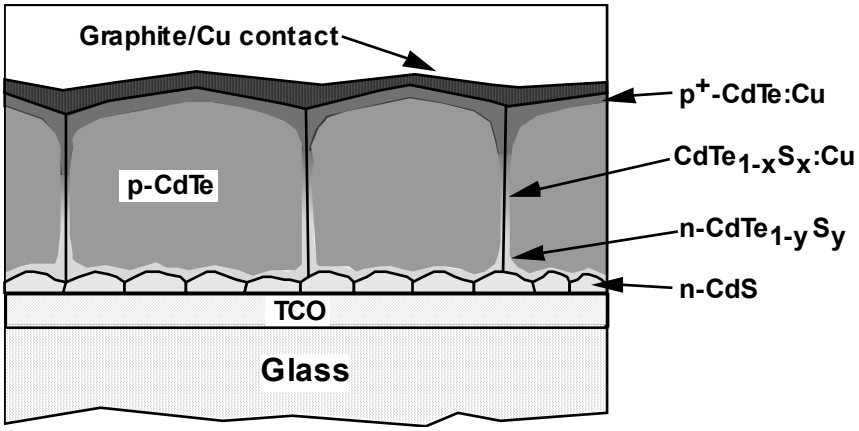

Figure 12 Polycrystalline CdS/CdTe schematic cross-section

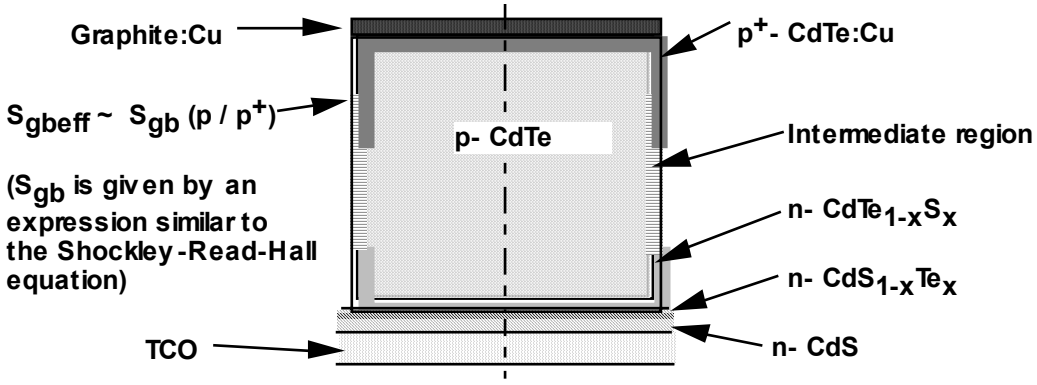

Figure 13 "Single grain" schematic cross-section, where S_{gb} is the recombination velocity at the grain boundary.

3.5 Input parameters

Input parameters for the one-dimensional case of Figure 11, treated in the following, may be roughly separated into two groups:

Group 1: Relatively well known, once structure is defined (e.g., thicknesses, band gaps).

Group 2: Not well known. It is likely that modeling will help determine the ranges of magnitude for these parameters, e.g., carrier densities (n, p), lifetimes (τ), front and back contact potential barrier height (Φ_c), and CdS/CdTe interface recombination.

For simplicity, in this series of simulations it is assumed that there is a Schottky diode at the back contact, there is no recombination at the CdS/CdTe interface, and there is no TCO layer. Also assumed are an

(approximately) AM1.5 spectrum, optical absorption data for PX CdS and CdTe[10] , and a lifetime model for recombination. The procedure employed has been to set as many as possible of the Group 1 variables according to experimental data and to use educated guesses for the rest. Effects of the Group 2 variables are then determined by studying the variations induced by changing one variable at a time. Some variable variations have rather small effects for the regions of parameter space of interest and can be set constant, while others are pivotal and will require some experimental verification other than just matching J_{sc}, V_{oc} and ff. Focusing on one region of the cell at a time (e.g., the back contact, where front layer variables should have little effect) helped to simplify the problem.

All modeling to date disregards effects of grain boundaries, except for the optical absorption coefficient data.

3.6 Modeling results

The first task was to try to match existing cell parameters (un-stressed cells) using a combination of published values (e.g., optical absorption), measured quantities (e.g., CdTe thickness, n and p), and best guesses (e.g., lifetimes), as shown in Figure 11. Target device parameters were 25 mA/cm^2 Jsc, 0.85 V Voc, 0.750 ff, and 15.8% power conversion efficiency.

Optimization was done with the aid of a set of output-variable trend plots (J_{sc}, V_{oc} and ff) for each input variable. These plots indicated that some input variables had little effect on one or two of the output variables, while others had an unexpectedly large effect. By varying parameters, especially the electron lifetime and the depletion layer width in the CdTe, a good fit for J_{sc} and ff for the unstressed cell was obtained. V_{oc}, however resisted attempts to independently reduce it to a commonly observed level. The fact that experimental Voc is lower than the modeled value indicates that another loss mechanism, such as CdS/CdTe interfacial recombination, should be incorporated into the model. (Specific calculated values were: 25 mA/cm^2 J_{sc}, 0.948 V V_{oc}, 0.752 ff and η_s = 16.2 % efficiency.)

3.6.1 Modeling results for the front contact and CdS layer

1. The lifetime in the CdS has little effect for any but the highest CdS doping levels because the high field there sweeps the carriers out before they can recombine. This suggests that there may be some contribution to J_{sc} from the CdS layer.
2. The surface recombination velocity at the contact/CdS interface also has little effect on J_{sc}. (Except for the case when the front contact barrier height is larger than the difference between the valence band and the Fermi level, in which case the electric field at the CdS/electrode interface is reduced or inverted.)
3. Increasing the CdS thickness (x_{CdS}) has virtually no effect on V_{oc} and ff, but J_{sc} decreased linearly over the range of x_{CdS} of 0.01 μm to 0.1 μm, as expected.
4. Decreasing the electron density in a 0.1 μm CdS layer from 10^{17} to 10^{15} cm^{-3} increased J_{sc} by 2 mA/cm^2. Again there is virtually no effect on V_{oc} and ff.

3.6.2 Modeling results for the CdTe layer

1. Decreasing the hole density in the CdTe layer adjacent to the CdS (5×10^{16} to 5×10^{14} cm^{-3}) causes a corresponding increase in depletion layer width from 0.16 to 1.55 μm and resulted in a 2 mA/cm^2 increase in Jsc, due to increased electric-field aided collection of photogenerated carriers. On the other hand, since this field is reduced by forward bias, for large depletion layer

widths, there was considerable decrease in light-generated current (J_L) with increasing bias, causing V_{oc} and ff to decrease. The efficiency decreased 1.5 percentage points over this range of depletion layer widths.

2. The other major controlling variable is the minority carrier lifetime (τ) which was increased over the rather narrow range from 0.8 to 3.2 x 10^{-10} sec (which corresponds to minority carrier diffusion lengths of roughly 0.1 to 0.2 μm.) resulting in increases in J_{sc} of +1.2 mA/cm^2 and V_{oc} of +0.11 V.

   Using simple analytic models, this range of lifetimes would correspond to J_{sc} values of only 10 to 15 mA/cm^2 for a cell with no appreciable electric field in the CdTe absorber layer. Since the J_{sc} in this simulation was close to 25 mA/cm^2, this indicates that the carrier collection is strongly augmented by the field built into the CdTe layer by the doping layers.

   The ff was relatively constant except at the ends of the τ range where the change was only ±0.022.

3.7 Prognosis and future work

3.7.1 1D Modeling

The largest hurdle to getting useful results from AMPS is dealing with the large number of variables involved and gaining some perspective of their effects. Once a satisfactory set of input variables is determined, it is relatively simple to find the effects of the variables, one at a time. While the analysis presented here used only three target quantities (J_{sc}, V_{oc} and ff) other, readily accessible experimental data such as spectral response and V_{oc} vs. temperature would allow the model to be considerably refined.

The priorities for next year are as follows:

1. Interface recombination at the "CdS/CdTe" junction will be added by inserting a thin (on the order of 0.01 μm) layer of CdTe with considerably smaller lifetime. Because of the growth morphology it is quite likely that the effective lifetime in the CdTe is considerably lower near the CdS/CdTe interface than at the back of the cell where the grains are larger. This should have the effect of maintaining J_{sc} while decreasing the V_{oc} to more reasonable values.
2. A TCO layer of tin oxide (SnO_x) will be added to the model and its thickness varied. The effect of changing the conduction band discontinuity at the SnO_x/CdS interface will be examined. Also, the effect of a two layer TCO, with the high rho part next to the CdS will be considered.
3. Interdiffusion of S and Te will be considered by inserting a Te-rich CdSTe alloy layer and focusing on the recombination loss, rather than the optical properties. As a first approximation, it will be assumed that everything is the same in the CdTe and it alloy, except the band gap.
4. Focusing on the CdTe and using a single layer (rather than the 3 layers now used), carrier densities and lifetimes will be varied. This should help quantify the extent of electric-field aided collection. The effect of variation of the CdTe layer thickness, for two back-contact barrier potentials (0 eV and 0.5 eV - enough to seriously distort the J-V characteristic) will be evaluated.
5. Some minor additional studies of the back contact barrier potential effects may be made.

3.7.2 2D Modeling

3.7.2.1 2D Modeling approach

Although much can be learned about the CdS/CdTe cell using 1D modeling, the addition of the effect of grain boundaries (GBs) in a realistic way is problematic because of the strong dependence on geometry. A cross section of a PX CdTe/CdS cell is shown in Figure 14A. In order to simulate the PX CdS/CdTe solar cell in 2D, information (at least qualitative) about the electronic properties of the grain boundaries is needed. Two dimensional simulation should be considerably more realistic, but it is also more complex, requiring more variables and the use of work stations rather than PCs.

Apparently, GBs are beneficial, as suggested by the high efficiencies obtained in the PX cells relative to their single crystal (SX) counterparts. PX cells have high J_{SC} and the quantum efficiency curves suggest that there is relatively little recombination in the back of the cell (i.e., a high effective minority diffusion length). This, in turn, suggests that the grain boundaries may be acting as minority carrier mirrors in the back of the cell, as shown in Figure 14B (the A-A' section), so that carriers are funneled to the center of each grain and on to the junction.

Some data about GB in "SX" CdTe exists, obtained from electronic measurements. For example, the GBs observed in p-CdTe[11] have GB state densities within the band gap of 10^{10} to over 10^{12} eV/cm^2 in the regions within ~ 0.4 eV of both band edges. The charge on these states produces GB barrier heights of ~ 0.2 to 0.7 eV in p-CdTe (with acceptor densities of 10^{16} to over 10^{17} cm^{-3}). Similar barrier heights are measured in PX CdTe films. These barrier heights are strongly reduced by illumination (e.g., from 0.7 in the dark to 0.2 eV illuminated for a PX sample). Since the hole transport across the GBs is dominated by thermionic emission over the barriers, the resistivity is strongly decreased by illumination and by increasing temperature. Further, EBIC images using thin metal Schottky barriers on bicrystals generally show the GBs as dark lines, indicating substantially higher recombination there. The dependence of resistivity on illumination and temperature, and the dark EBIC signature are also observed in polycrystalline thin films. From the qualitative aspects of these data we can extrapolate to the band diagrams shown in Figure 14B. In addition, GB barrier heights can be reduced temporarily (weeks) by annealing p-CdTe in H_2 and n-CdTe in air[11].

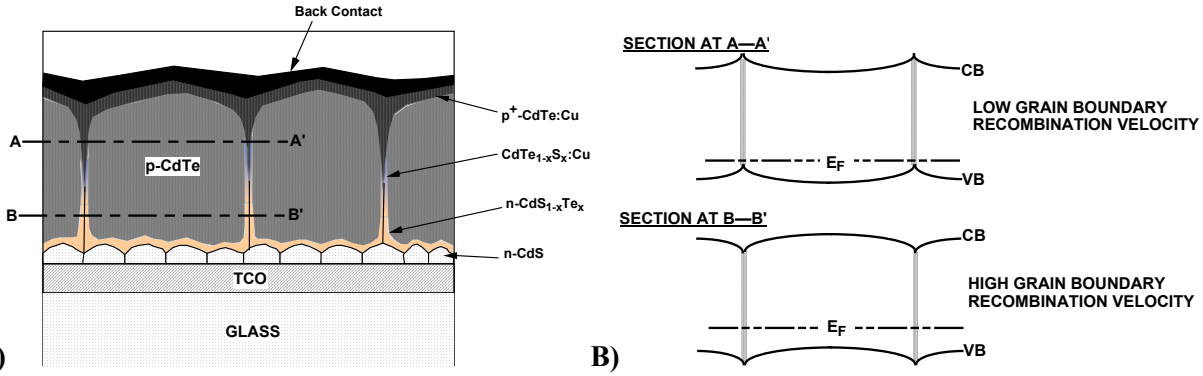

Figure 14 A) Proposed cross section of a CdS/CdTe solar cell. B) Band diagrams for the cell shown at two planes parallel to the junction plane. In section A-A' copper diffusion down the GB has made them more p-type and the resultant band bending tends to force light-generated electrons away from the GB.

3.7.2.2 Planned experiments

Below are a series of experiments that promise to give much information about the activity of grain boundaries (GB) in CdTe-based solar cells. While the simple experiments outlined below will certainly

not give a complete picture, they will make a large contribution to qualitative understanding of Cu-diffused GB. The bicrystals are readily available and the PX CdTe films on insulating substrates should be easy to make as add-ons during regular solar cell fabrication runs. These experiments should give qualitative results on:

1. Cu diffusion induced carrier profiles in CdTe
2. Cu diffusion induced resistivity in CdTe
3. GB barrier heights and state densities of both SX and PX GB
4. conductivity in the plane of Cu-diffused GB
5. speed of Cu diffusion along GB
6. recombination properties of both SX and PX GB.

3.7.2.2.1 Bicrystal grain boundary characterization procedure

Step 1. Chem-polish top of p-CdTe bicrystal. Cut in half across GB.

Step 2. Deposit Cu on part A. Heat treat. Etch off metallic copper. (Figure 15).

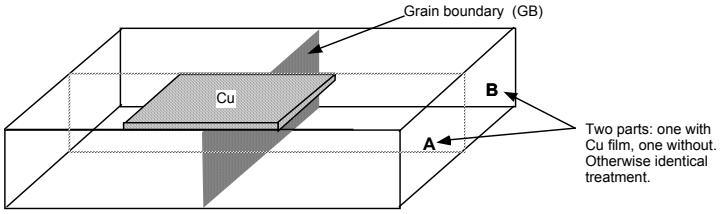

Figure 15 Cu film deposited over a portion of a grain boundary (Step 2).

Step 3. Add Indium Schottky barriers and gold semi-ohmic contacts.

Step 4 Do capacitance-voltage (C-V) on Cu diffused part compared with no-Cu part to get carrier densities and profiles (Figure 16).

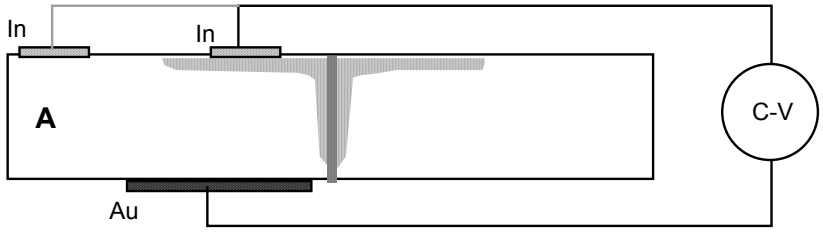

Figure 16 In and Au electrode placement on bicrystal for C-V measurements (Step 4).

Step 5 Do four-point I-V to determine resistivity on both Cu-doped and undoped portions (Figure 17).

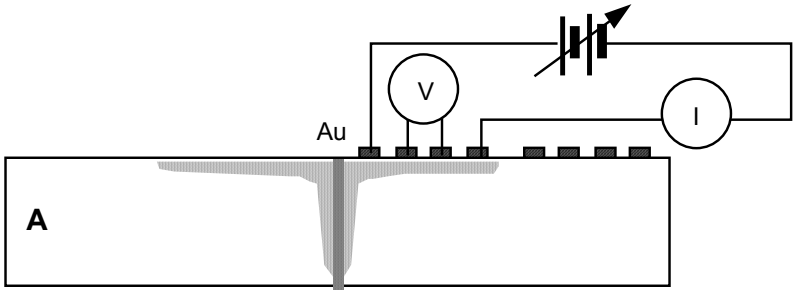

Figure 17 Four point measurement locations on Cu-diffused and un-doped CdTe crystal surfaces (Step 5).

Step 6 Measure four-point resistivity measurement to verify that resistivity is the same for part without Cu (Figure 18).

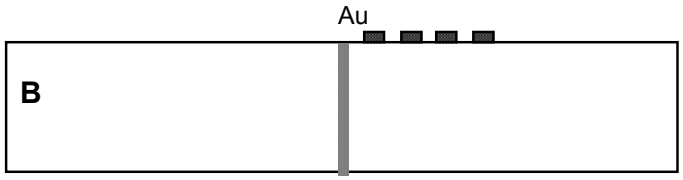

Figure 18 Four point probe placement on un-doped crystal near grain boundary (Step 6).

Step 7 Measure four-point I-V to determine grain boundary state density without Cu doping of GB with and without illumination (Figure 19). Also measure C-V across the GB in the light and in the dark. Temperature dependence of the I-V (around room temperature) gives a measure of the GB barrier height.

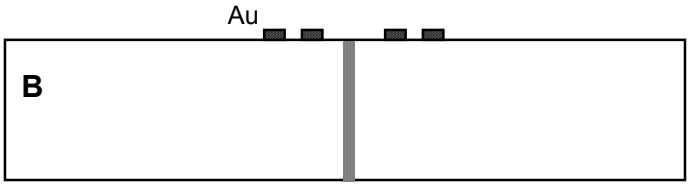

Figure 19 Four point probe placement for I-V and C-V characterization of un-doped grain boundary (Step 7).

Step 8 Lap and/or etch off Cu diffused top layer.

Step 9 Measure four-point I-V vs. temperature to determine grain boundary barrier height and state density with Cu doping of GB (with and without illumination). Also C-V across the GB in the light and in the dark.

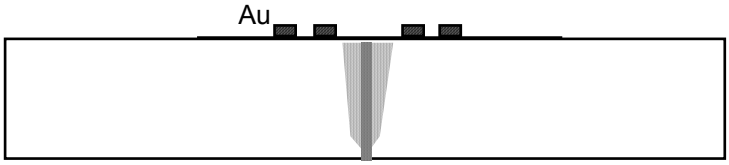

Figure 20 Four point probe placement for I-V and C-V characterization of Cu-doped grain boundary (Step 9).

Step 10 Etch off contacts. Thin bicrystal A from the back.

Step 11 Measure 2 point I-V to determine grain boundary conductivity with and without Cu doping of GB - with and without illumination (Figure 21).

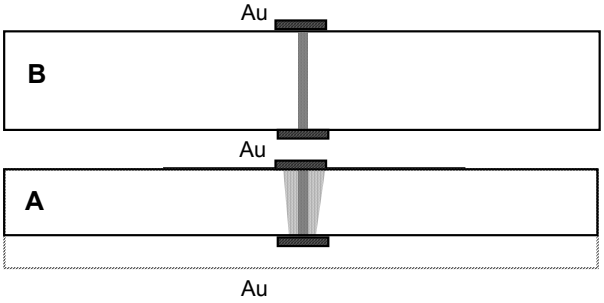

Figure 21 Electrode placements for measuring grain boundary conductance (Step 11).

Step 12. Etch off and re-apply thin contacts for EBIC.

Step 13 Perform scanning EBIC and cathodoluminesence to help determine recombination effects of GB with and without Cu doping - with and without illumination (Figure 22).

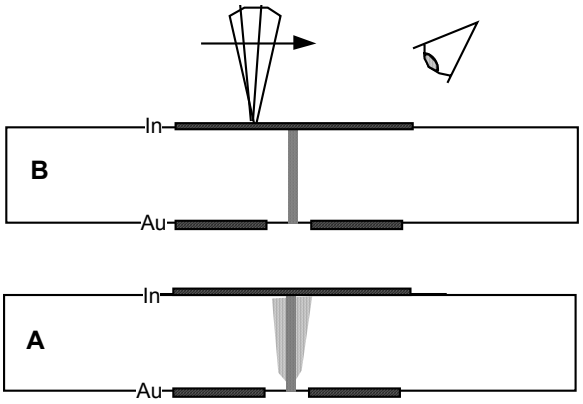

Figure 22 Electrode placement and electron beam scan location for ebic / cathodoluminescence measurements (Step 13).

Note: The same experimental series might be done 1) with $CdCl_2$, 2) with both Cu and $CdCl_2$, 3) with CdS and a $CdCl_2$ heat treatment, and 4) with CdS and heat treatment followed by Cu diffusion.

3.7.2.2.2 Polycrystalline film grain boundary characterization

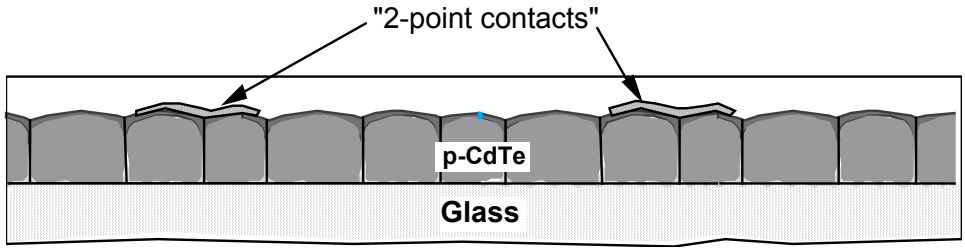

Figure 23 Electrode placement for in-plane resistivity measurements on polycrystalline thin films.

Another possible group of experiments would use PX CdTe films on 7059 glass with Cu and/or $CdCl_2$ or with CdS and $CdCl_2$ heat treatment and/or Cu diffusion. In this case, the resistance across the film, light and dark, as a function of temperatures should give barrier heights. Figure 23 shows the electrode placement. Light to dark decay time should give a measure of the effective recombination lifetime at the grain boundary (much like surface photovoltage decay, including time domain magnification because of depletion layer charge).

4 Summary

4.1 First year accomplishments

During the first year of the program the concept of APCVD of CdTe has undergone rigorous evaluation by the combined ITN/CSM scientific and engineering team and the apparent practical advantages of APCVD over state-of-the-art manufacturing techniques have stood up under this scrutiny. Nonetheless, at the end of year one of the program APCVD's apparent advantages have not yet been demonstrated.

Real progress has been made, however. The APCVD reactor has been designed and built and shake-down testing is in progress. The reactor appears to be *almost* ready for demonstration and experimental evaluation of APCVD's apparent advantages.

In addition, groundwork has been laid for development of experiment-based, two-dimensional modeling of polycrystalline thin film CdTe PV devices. One-dimensional modeling has demonstrated the ability to reproduce the essential characteristics of polycrystalline CdTe PV device performance and a detailed plan for measurement of grain boundary characteristics has been established.

Specific accomplishments of the first year of the APCVD subcontract include:

- Selection of the Stagnant Flow Reactor design concept
- Development of a detailed reactor design
- Performance of detailed numerical calculations simulating reactor performance
- Fabrication and installation of APCVD reactor
- Performance of dry runs to verify reactor performance
- Performance of one dimensional modeling of CdTe PV device performance
- Development of a detailed plan for quantification of grain boundary effects in polycrystalline CdTe devices

4.2 Planned second year milestones

During the second year of the program ITN expects to meet the following milestones as called for in the original subcontract:

- Demonstration of device quality CdTe films.
- Demonstration of 12% power conversion efficiency.
- Presentation of two-dimensional methods for characterization and analysis of device operation on a microscopic scale.

5 Major articles published during Phase I of the subcontract

P. Meyers, R. Kee, L. Raja, C. Wolden and M. Aire, "Atmospheric Pressure Chemical Vapor Deposition of CdTe – Reactor Design Considerations", CP462, NCPV Photovoltaics Program Review, edited by M. Al-Jassim, J.P. Thornton, and J.M. Gee, (1998) pp 218-223.

P. Meyers "Development of Thin Film PV Devices", Technical Digest Twelfth "Sunshine" Workshop on Thin Film Solar Cells (1999), organizer M. Konagai (Tokyo Inst. Tech.) MITI, Japan pp77-84.

6 References

1 P.V. Meyers and R.W. Birkmire, Prog. in PV:Res. & Appl., Vol 3 (1995) pp 393-402.

2 C. Ferekides and J. Britt, Solar Energy Mat. & Solar Cells 35 (1994) pp 255-262.

3 H. Ohyama, T. Aramoto, S. Kumazawa, H. Higuchi, T. Arita, S. Shibutani, T. Nishio, J. Nakajima, M. Tsuhi, A. Hanafusa, T. Hinino, K. Omura, and M. Murozono, "16.0% Efficient Thin-Film Solar Cells", Proc. 26th PVSC (1997) pp 343-346.

4 T.C. Anthony, A.L. Fahrenbruch, and R.H. Bube, J. Vac. Sci. Technol. A 2 (3), (1984), pp 1296-1302.

5 K. Mitchell, C. Eberspacher, F. Cohen, J. Avery, G. Duran and W. Bottenberg, "Progress towards high efficiency, thin film CdTe solar cells", Proc 18th IEEE PVSC (1985) pp 1359-1364.

6 C. J. Geankopolis, Transport Processes and Unit Operations, 2nd Ed., (Allyn and Bacon, Inc., Boston, 1983) Chapter 7.
7 AMPS-1D is a one-dimensional semiconductor transport computer simulation program written under the direction of Prof. S. Fonash at Pennsylvania State University, with the support of the Electric Power Research Institute.
8 Also see A. Fahrenbruch, "Modeling of Polycrystalline Thin Film Solar Cells," NCPV Photovoltaics Program Review, Proc. of 15th Conf., Sept. , 1998, Denver, CO. AIP Conf. Proc. vol. 462, p. 48.
9 James Sites, Annual Report, CSU, 3/99.
10 Optical absorption data was obtained from D. Albin at NREL (1997).
11 T. Thorpe et al., J. Appl. Phys. **60**, 3622 ('86)

REPORT DOCUMENTATION PAGE

Form Approved
OMB NO. 0704-0188

1. AGENCY USE ONLY (Leave blank)	2. REPORT DATE	3. REPORT TYPE AND DATES COVERED
	September 1999	Annual Report, 26 January 1998–25 January 1999

4. TITLE AND SUBTITLE
Atmospheric Pressure Chemical Vapor Deposition of CdTe for High-Efficiency Thin-Film PV Devices; Annual Report, 26 January 1998–25 January 1999

5. FUNDING NUMBERS
C: ZAK-8-17619-03
TA: PV905001

6. AUTHOR(S)
P.V. Meyers, R. Kee, C. Wolden, L. Raja, V. Kaydanov, T. Ohno, R. Collins, M. Aire, J. Kestner, A. Fahrenbruch

7. PERFORMING ORGANIZATION NAME(S) AND ADDRESS(ES)
ITN Energy Systems
12401 West 49th Ave.
Wheat Ridge, CO 80033

8. PERFORMING ORGANIZATION REPORT NUMBER

9. SPONSORING/MONITORING AGENCY NAME(S) AND ADDRESS(ES)
National Renewable Energy Laboratory
1617 Cole Blvd.
Golden, CO 80401-3393

10. SPONSORING/MONITORING AGENCY REPORT NUMBER
SR-520-26566

11. SUPPLEMENTARY NOTES
NREL Technical Monitor: H.S. Ullal

12a. DISTRIBUTION/AVAILABILITY STATEMENT
National Technical Information Service
U.S. Department of Commerce
5285 Port Royal Road
Springfield, VA 22161

12b. DISTRIBUTION CODE

13. ABSTRACT *(Maximum 200 words)*
ITN's 3-year project, titled "Atmospheric Pressure Chemical Vapor Deposition (APCVD) of CdTe for High-Efficiency Thin-Film Photovoltaic (PV) Devices," has the overall objectives of improving thin-film CdTe PV manufacturing technology and increasing CdTe PV device power conversion efficiency. CdTe deposition by APCVD employs the same reaction chemistry as has been used to deposit 16%-efficient CdTe PV films, i.e., close-spaced sublimation, but employs forced convection rather than diffusion as a mechanism of mass transport. Tasks of the APCVD program center on demonstrating APCVD of CdTe films, discovering fundamental mass-transport parameters, applying established engineering principles to the deposition of CdTe films, and verifying reactor design principles that could be used to design high-throughput, high-yield manufacturing equipment. Additional tasks relate to improved device measurement and characterization procedures that can lead to a more fundamental understanding of CdTe PV device operation, and ultimately, to higher device conversion efficiency and greater stability. Specifically, under the APCVD program, device analysis goes beyond conventional one-dimensional device characterization and analysis toward two-dimension measurements and modeling. Accomplishments of the first year of the APCVD subcontract include: selection of the Stagnant Flow Reactor design concept for the APCVD reactor, development of a detailed reactor design, performance of detailed numerical calculations simulating reactor performance, fabrication and installation of an APCVD reactor, performance of dry runs to verify reactor performance, performance of one-dimensional modeling of CdTe PV device performance, and development of a detailed plan for quantification of grain-boundary effects in polycrystalline CdTe devices.

14. SUBJECT TERMS
photovoltaics ; atmospheric pressure chemical vapor deposition ; APCVD ; cadmium telluride ; CdTe ; reactors ; device performance ; thin films ; high efficiency ; modeling

15. NUMBER OF PAGES

16. PRICE CODE

17. SECURITY CLASSIFICATION OF REPORT	18. SECURITY CLASSIFICATION OF THIS PAGE	19. SECURITY CLASSIFICATION OF ABSTRACT	20. LIMITATION OF ABSTRACT
Unclassified	Unclassified	Unclassified	UL